Clock pulse modulation for ripple reduction in buck-converter circuits

Daisuke Ito[a,*], Hiroyuki Asahara[b], Takuji Kousaka[c], Tetsushi Ueta[d]

[a]*Department of Electrical, Electronic and Computer Engineering, Gifu University, 1-1 Yanagido Gifu, Gifu, 501-1193, Japan*
[b]*Department of Electrical and Electronic Engineering, Faculty of Engineering, Okayama University of Science, 1-1 Ridai-cho, Kita-ku Okayama-shi, Okayama, 700-0005 Japan*
[c] *Energy Conversion Engineering, Department of Mechanical and Energy Systems Engineering, Faculty of Engineering, Oita University, 700 Dannoharu, Oita 870-1192, Japan*
[d]*Center for Administration of Information Technology, Tokushima University, 2-1 Minamijyousanjima-cho Tokushima, Tokushima, 770-8506, Japan*

Abstract

DC-DC switching converters which are frequently treated as hybrid dynamical systems exhibit complex behavior due to nonlinear and interrupt characteristics. For synchronous buck-converters, we propose a method to control chaotic behavior by pulse-frequency modulation. An input voltage, a duty ratio of PWMs, and so on, affect to the regulation characteristics of converters directly, but a frequency of PWMs is determined by the frequency characteristics of the converter and is set as a fixed value. The proposed chaos-control method suppresses chaotic responses by slightly perturbing the pulse frequency alone, therefore our method can stabilize unstable periodic orbits without influence on the voltage regulation scheme. To simplify the feedback controller, the condition of dimension reduction for the controlling gain vector is derived. The proposed controller acheves the stabilization without a current sensor. Numerical simulation and circuit implementation demonstrate the validity of this method.

Keywords: Controlling chaos, buck converter, pulse-frequency modulation

*Corresponding author
Email addresses: d_ito@gifu-u.ac.jp (Daisuke Ito), asahara@bifurcation.jp (Hiroyuki Asahara), takuji@oita-u.ac.jp (Takuji Kousaka), ueta@tokushima-u.ac.jp (Tetsushi Ueta)

1. Introduction

Electrical circuits with switches are frequently treated as hybrid dynamical systems [1, 2]. They occur in many engineering fields [3, 4]. Hybrid dynamical systems have some deterministic flows and flip these flows in a non-smooth manner with discrete events. This nonlinearity causes rich complex behavior such as bifurcation phenomena and chaotic attractors [3]. Saito et al. have found chaotic attractors in one-dimensional *piecewise linear* systems [5, 6, 7], and they have validated the presence of bifurcation phenomena and chaotic attractors with explicit solutions.

High-power circuits can inevitably be treated mathematically as hybrid systems since the electrical switches, relays, and MOS-FETs may cause non-smooth and interruptive characteristics determined by discrete events [8, 9]. DC-DC converters are practically used as DC voltage converters, in fact, such switching converters are also categorized as hybrid systems, and their bifurcations and chaotic attractors have been analyzed thoroughly [10, 11]. Waveforms of these circuits looks noisy [12], indeed, they show pseudo-random and continuous-spectrum characteristics. From the viewpoint of converter performance, the noise-like responses increase ripple voltages and electromagnetic interference.

While, controlling chaos is an effective method to suppress the chaotic responses [13, 14]. In recent studies, various control schemes have been proposed [15, 16, 17, 18]. These authors achieved ripple reduction by stabilizing previously unstable periodic orbits (UPOs). Yan-Li et al. proposed a control method for buck converters that varies the source voltage [19]. The frequency domain information is applied for the controlling chaos for boost converters by Rodríguez et al.[20], and suppressing chaotic behavior is successfully achieved. In the stability analysis utilizing Monodromy matrices [21], it suggests that an interrupt characteristic is important for the circuit behavior. Poddar et al. [22] proposed the controlling chaos method utilizing the switching characteristics of a buck converter circuit, and we also proposed the method that varies switching threshold values as reference voltages [16]. As these studies, the stabilization schemes using switching characteristics for converter circuits have achieved good controlling performance, but they require the load current value, which is difficult to measure precisely

for the state-feedback, and treated only simple circuit models, indeed, an inductor is often omitted in a mathematical model. Additionally, circuit configurations including input and output voltages, loads, and reference values are not easy to be changed dynamically because they are determined by the converter specifications and usage.

On the other hand, a pulse width modulation (PWM) input is often used to drive the converter circuit. Its duty ratio depends on requested values and the output voltage, whereas the optimum period of the pulse is determined by the frequency characteristics of a converter. An output voltage controller for a DC-DC converter adjusts the duty ratio to deal environmental, source voltage, and requested output voltage changes. In contrast, the frequency is usually considered as a fixed value, while it composes a PWM generator; we mean that it is independent on the converter circuits, so it is easy to adjust by other controllers. The chaos control with small-signal inputs has also been proposed [23, 24, 25], and Kikuchi et al. proposed a frequency modulation method that offers the possibility of controlling chaos in practical systems for a semiconductor laser [26]. On the viewpoint of a DC-DC converter, the controller with pulse frequency modulation can suppress chaotic phenomena with the small frequency perturbation of PWMs. For all of these reasons, a frequency modulation for the controlling chaos will be available in combination with an output voltage controller, and it can reduce ripple voltages without influence for the performance of the voltage conversion.

In a previous study, we proposed chaos control in a buck converter with PWM [27]. However, target circuit is an identical model that omits an inductor and operates under light-loads. In this paper, we expand our method for an actual circuit model and propose a simplification of the controller. We report our attempt to suppress chaotic phenomena in a synchronous buck-converter circuit through pulse width (frequency) modulation of a clock. The frequency of the PWM is perturbed based on feedback control. The controlling gain was designed with a pole-assignment method [28], and the stability of circuits with the proposed controller can be proved accordingly. To achieve the voltage feedback controller without current measurements, we employ the condition for poles on which controlling gain vectors degenerate. Whereas, it is unclear the relationship between responsiveness and robustness and the controller designed by a pole-assignment method, but this problem will avoid by using optimal control the-

ory. First, we explain the circuit model and the design procedure for the feedback gain. Next, we demonstrate the performance of the proposed method with numerical simulations, and the simulated results reveal the robustness of the proposed method. Finally, to confirm feasibility of the method and applicability to real circuits, a prototype controller is configured for a sample buck-converter. We show its laboratory experiment results.

2. Circuit model and analytic results

Let us consider the synchronous buck-converter circuit diagrammed in Fig. 1. Two switches have zero resistance when ON and infinite resistance when OFF, without a time delay. The switches are flipped according to a rule that depends on the output voltage v_o and the clock with the period time T. The PWM generator and the error amplifier comprise a general voltage-mode controller. If we assume that v and i are state variables, the normalized equation is given in Eq. (1).

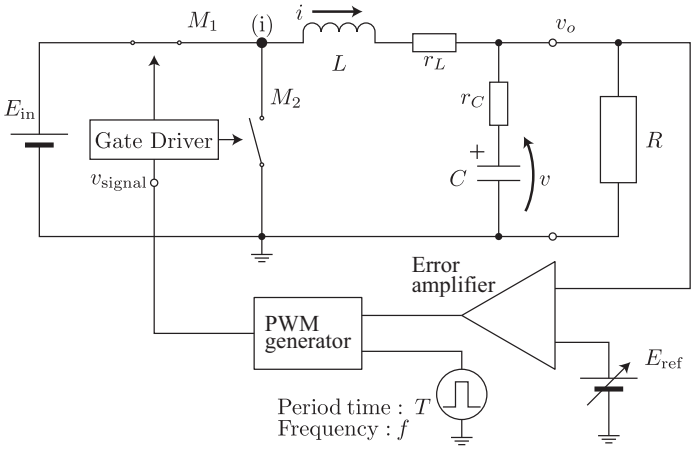

Figure 1: Synchronous buck-converter circuit with a voltage-mode controller.

$$\begin{aligned} \frac{dx}{dt} &= -\beta x + \alpha y \\ \frac{dy}{dt} &= -\alpha x - \gamma y + e \end{aligned} \tag{1}$$

where

$$t = \frac{1}{\sqrt{LC}} t', \quad x = \sqrt{\frac{C}{L}} v, \quad y = i \tag{2}$$

and

$$\rho = \frac{1}{\sqrt{LC}}T, \quad \alpha = \frac{R}{R + r_c}, \quad \beta = \frac{1}{R + r_c}\sqrt{\frac{L}{C}},$$
$$\gamma = \left(r_L + \frac{Rr_c}{R + r_c}\right)\sqrt{\frac{C}{L}}, \quad e_{\text{in}} = \sqrt{\frac{C}{L}}E_{\text{in}}, \quad e_{\text{ref}} = \sqrt{\frac{C}{L}}E_{\text{ref}}. \tag{3}$$

Note that the symbol e in Eq. (1) is the normalized voltage at point (i) in Fig 1 and is set to e_{in} or zero for the two switches. The voltage-mode controller supplies v_{signal}. The reference voltage E_{ref} determines the output voltage. The error amplifier compares the output voltage with E_{ref}, and provides the duty ratio to the PWM generator. The two switches M_1 and M_2 are driven exclusively by the gate driver. M_1 switches ON once in every period T driven by clock pulses, after which the input supply E_{in} flows to the load. When the output voltage v_o is larger than the reference voltage E_{ref}, M_2 is switched ON, and the voltage supply is cut off. In terms of the capacitance C and its series resistance r_C, the output voltage can be described as $v_o = v + r_c C dv/dt$. Consequently, the switching rules are as follows:

- if the time $t = n\rho$ then $e = e_{\text{in}}$,
- if $x > ay + b$ then $e = 0$,

where

$$a = -r_c\sqrt{\frac{C}{L}}, \quad b = \frac{R + r_c}{R}\sqrt{\frac{C}{L}}E_{\text{ref}}. \tag{4}$$

Following Eq. (1), the dynamical system is composed of linear ordinary differential equations, but the parameter e changes discontinuously depending on states and the time. The interruptive event is strongly nonlinear. The buck converter expresses various phenomena depending on resistor loads and frequencies of the PWM signals. The chaotic attractor is shown in Fig. 2 (a). This plot confirms that the ripple in the state x is about 0.5V. Figures 2 (b) and (c) are 1-period and 2-period UPOs embedded into the chaotic attractor, respectively. Their ripple voltages are smaller than the chaotic attractor. Therefore, the ripple voltages will be decreased if the UPOs are stabilized by appropriate control inputs.

We obtain the bifurcation diagram in Fig. 3 by solving the fixed-point problem derived from the periodic orbit with suitable Poincare mapping [29, 30]. The curves

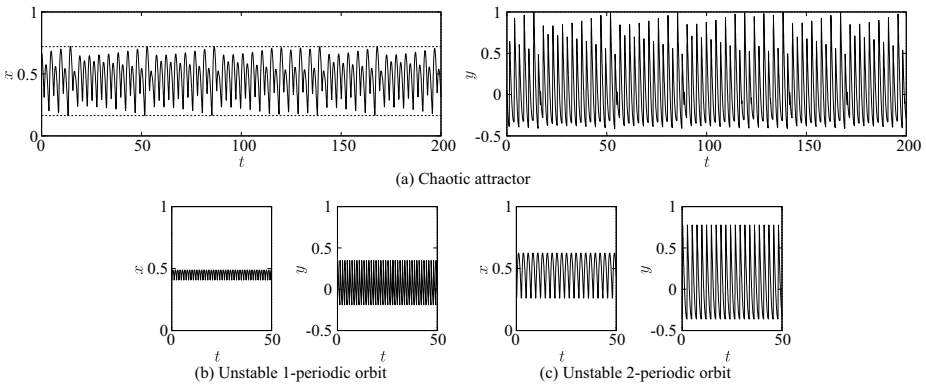

Figure 2: Chaotic attractor and unstable periodic orbits. The ripples of capacitor voltages and inductor currents on UPOs are obviously smaller than the chaotic attractor. ($\alpha = 0.995$, $\beta = 0.1$, $\gamma = 0.7281$, $e_{\text{in}} = 5.372$, $\rho = 1.2$, $a = -0.2238$ and $b = 0.517$).

labeled PD and BC are the period doubling and border-collision bifurcations, respectively. Note that, the index number of each symbol indicates the period, and dashed lines are bifurcation parameter sets for UPOs. Chaotic attractors appear inside of PD^1 and PD^2, and two types of attractors occur. In the 3-period region, 3-periodic and chaotic attractors coexist, and The 1-periodic and 2-periodic attractors are coexist in the shaded region between BC^2 and PD^1. They depend on initial values.

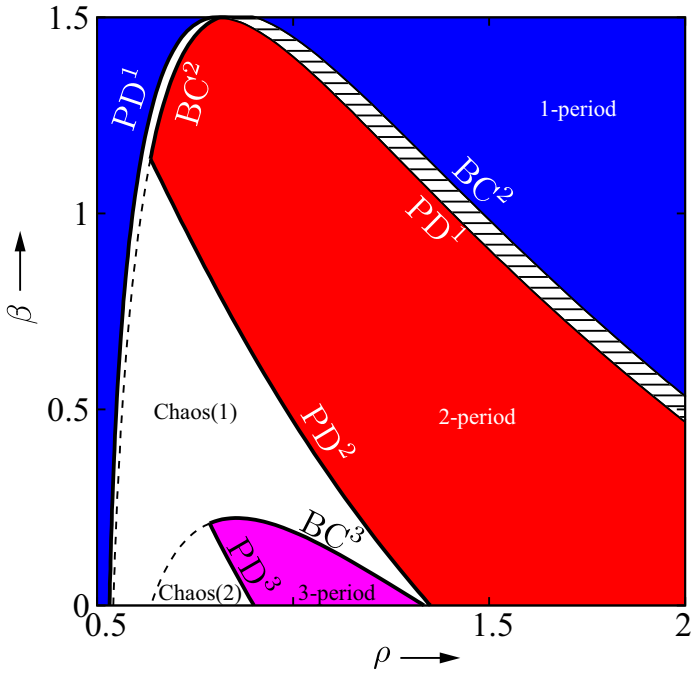

Figure 3: Bifurcation structures of the buck converter. The horizontal and vertical axes are related to the frequency of the PWM and the load resistor, respectively. The symbols BC and PD are border-collision and period doubling bifurcations. Their index numbers show the period.

3. Control method: pulse-frequency modulation to stabilize UPOs

We propose the following control scheme to stabilize UPOs with appropriate feedback. The pole-assignment method helped us design the appropriate feedback gain. Let us consider the following discrete-time dynamical system:

$$\boldsymbol{x}_{k+1} = \boldsymbol{F}(\boldsymbol{x}_k,\ \lambda),\ \boldsymbol{x} \in \boldsymbol{R}^n,\ \lambda \in \boldsymbol{R}. \tag{5}$$

If $\boldsymbol{x}^* = \boldsymbol{F}^m(\boldsymbol{x}^*,\ \lambda)$ is satisfied then the initial state $\boldsymbol{x}^*$ is called the m-period point. Assuming a control input $u_k = G(\boldsymbol{x}^* - \boldsymbol{x}_k)$ for the parameter, the system is described as $\boldsymbol{x}_{k+1} = \boldsymbol{F}(x_k,\ \lambda + G(\boldsymbol{x}_k - \boldsymbol{x}^*))$, where $G \in \boldsymbol{R}^n$ is the controlling gain. Thus, the characteristic equation for small perturbations around $\boldsymbol{x}^*$ is shown as follows:

$$\chi(\mu) = \det\left(A + BG - \mu I\right) = 0, \tag{6}$$

where

$$A = \frac{\partial \boldsymbol{F}}{\partial \boldsymbol{x}^*} \in \boldsymbol{R}^{n\times n},\ B = \frac{\partial \boldsymbol{F}}{\partial \lambda} \in \boldsymbol{R}^n, \tag{7}$$

and I is the unity matrix. Generally, the derivation of a Poincaré map and its derivatives is difficult because hybrid dynamical systems have discontinuous or non-smooth characteristics. However, a computation process using local maps and their compositions has already been proposed [30], and these maps can be computed numerically. Next, we consider the 2-dimensional dynamical equations, so we obtain

$$\chi(\mu) = \mu^2 - p\mu + q = 0, \tag{8}$$

where p and q are the control parameters that indicate the pole of multipliers μ_i. If the system behaves as the objective periodic solution $\boldsymbol{x}^*$, then the condition of its stability is expressed as $|\mu_i| < 1$. Thus the modulus of μ_i is less than unity if p and q are placed in a triangle such that:

$$q < 1, \quad q - p + 1 > 0, \quad q + p + 1 > 0. \tag{9}$$

In an electrical circuit with inductors, the behavior of electrical currents is included in the state variables. This condition raises a problem for state-feedback control since current measurement requires a shunt resistor or an expensive current probe. Therefore,

let us consider the option of dimension reduction to the controlling gain vector G to eliminate y from the definition of control inputs $u(k)$. In the variable transformations in Eq. (3), the state variables x and y correspond to the voltage and current, respectively. Thus, we derive the p-q condition of $g_1 = 0$. From this assumption, the variational equation can be described as follows:

$$\mu^2 - (a_0 + a_3 + b_0 g_0)\mu - (a_1 + b_1 g_0)a_2 = 0, \tag{10}$$

where

$$A = \begin{pmatrix} a_0 & a_2 \\ a_1 & a_3 \end{pmatrix}, \; B = \begin{pmatrix} b_0 \\ b_1 \end{pmatrix} \text{ and } G = \begin{pmatrix} g_0 \\ g_1 \end{pmatrix}, \tag{11}$$

so that

$$a_0 + a_3 + b_0 g_0 = p, \tag{12}$$

$$-(a_1 + b_1 g_0)a_2 = q. \tag{13}$$

Equation (12) is solved for g_0, and then the controlling gain is

$$g_0 = \frac{1}{b_0}(p - a_0 - a_3). \tag{14}$$

We obtain the relational equation between p and q as

$$q = a_2 \frac{b_1}{b_0} p - a_1 a_2 + a_2 \frac{b_1}{b_0}(a_0 + a_3). \tag{15}$$

As a result, Eqs. (9) and (15) are conditional equations driving the objective trajectories to stability, and g_1 is zero. Figure 4 plots the stabilizable p-q regions. Hence, by setting the control parameter on the line ℓ, the objective trajectories can be stabilized with only information limited expressed with the variable x.

In the target circuit model, various controlling schemes are proposed. Kousaka et al., for example, have used the source voltage E, and we have also proposed a control scheme with the threshold value E_{ref}. On the other hand, the frequency f of the clock pulse input is also adjustable, if we implement voltage-controlled oscillators. The duty ratio of the clock influences the output voltage directory, but its period is of little relevance. However, the period is an important parameter for the behavior in the circuit,

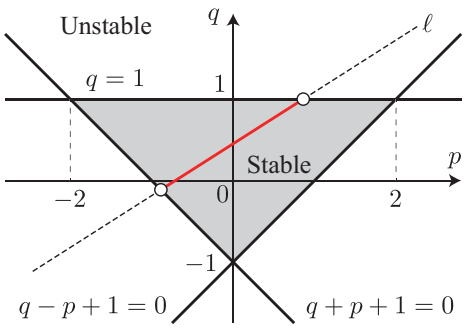

Figure 4: Sketch of stability in the p-q plane. The line ℓ is drawn by Eq. (15). One can obtain the controlling gain with $g_1 = 0$ by setting p and q on this line.

and could be an efficient control parameter. Next, we explain specific control schemes that perturb the period.

Figure 5 shows the voltage waveform for the pulse-frequency modulation (PFM) control method, where T is the period of the clock pulse. This trajectory means the capacitor voltage is equivalent to the output voltage. At first, the switch M_1 is in the ON state and the capacitor is charged up by the input source E. When v reaches the reference voltage E_{ref}, the signal turns the switches to the OFF state. The clock pulse can reset the behavior of the circuit. If the pulse is added at OFF state, the signal returns to the ON state. Repeating these two phases, the buck converter can regulate input voltages to required output voltages. Our proposed method perturbs the period T of the clock signal. Figure 5 confirms that the point v_{k+1} shifts to a lower value by the extension of the pulse width $T + u(k)$; thus the system state v_k can be controlled by adjusting the pulse width. This is one kind of PFM. Hence, the proposed method can stabilize UPOs without an influence on the voltage regulation scheme, based on voltage-mode control.

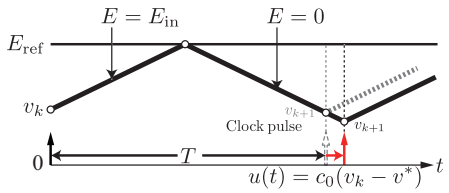

Figure 5: Frequency modulation of a clock pulse for the controlling chaos.

4. Numerical simulation results

From the control parameters in Eqs. (9) and (15), the range of p can be derived. The ranges of the 1-period and 2-period UPOs are $(-1.07,\ 1.17)$ and $(-1.048,\ 1.141)$, respectively. In this case, the controlling gain g_0 which corresponds to p can be derived by Eq. (14). They are listed in Table 1.

Table 1: Replaced poles and controlling gains ($g_1 = 0$).

1-period UPO
$-1.326 < p < 0.9864,\ -0.0136 < q < 0.326$ $-12.37 < g_0 < -2.282$
2-period UPO
$-1.099 < p < 1.089,\ 0.08917 < q < 0.09886$ $-2.914 < g_0 < -0.08874$

Figure 6 shows the control results. The waveforms represent the capacitor voltage x and the inductor current y. The 3rd figure for each result is a controlling signal $u(t)$. Figure 6 (a) confirms that the capacitor voltage exceeds the specified amount at the beginning. However, this voltage returns to the objective value e_{ref} as the control input value $u(t)$ decreases. Finally, the voltage converged to a 1-period orbit with small ripples. Figure 6 (b) shows that the system also converged to an objective 2-period attractor, and the control signal goes to zero. These results demonstrate that the proposed method can control the system with clock pulse modulation and can stabilize objective UPOs with a finite control input. Figure 7 shows the response of each result over a long period of time. Note that the frequency modulation for the stabilization of UPOs stops at $t = 600$ and after that the model is driven only by the voltage-mode controller. These results confirm that the behavior of the model returns to chaotic attractors after the stabilization of UPOs ceases.

To investigate the robustness of the controller, basins of attraction were computed as shown in Fig. 8. Each axis is the initial state $\boldsymbol{x}(0)$, and the strengths of colors indicate the unsuccessful or the convergence time of the control scheme. This result confirms that the model can converge to UPOs from nearly initial states in a time smaller than 50s. Thus the proposed method can stabilize UPOs not only from an initial configuration but also on-line. Note that in the 2-periodic UPO, a fractal-like structure appears.

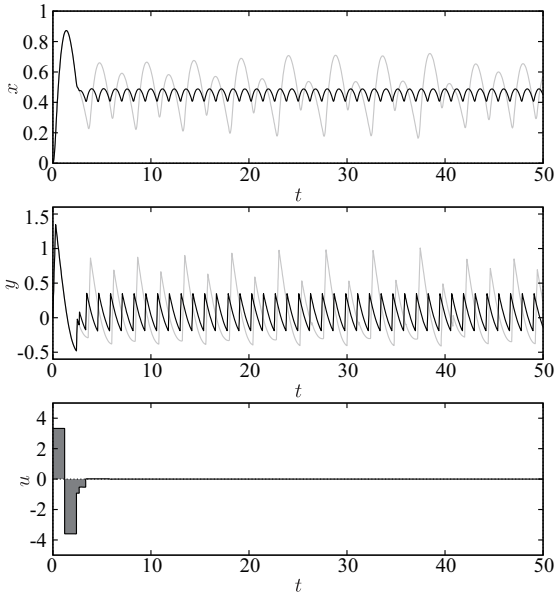

(a) 1-period orbit
$(x_0,\ y_0) = (0.4125,\ -0.1889)$, $(p,\ q) = (0, 0.1313)$ and $g_0 = -8.068$.

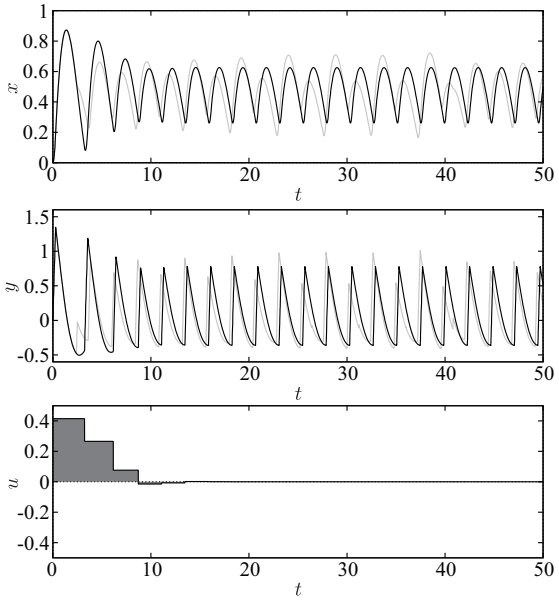

(b) 2-period orbit
$(x_0,\ y_0) = (0.2753,\ -0.3615)$, $(p,\ q) = (0, 0.09399)$ and $g_0 = -1.507$.

Figure 6: Control results for two UPOs. The waveforms converge to the target periodic orbits, and the control inputs $u(t)$ become zero.

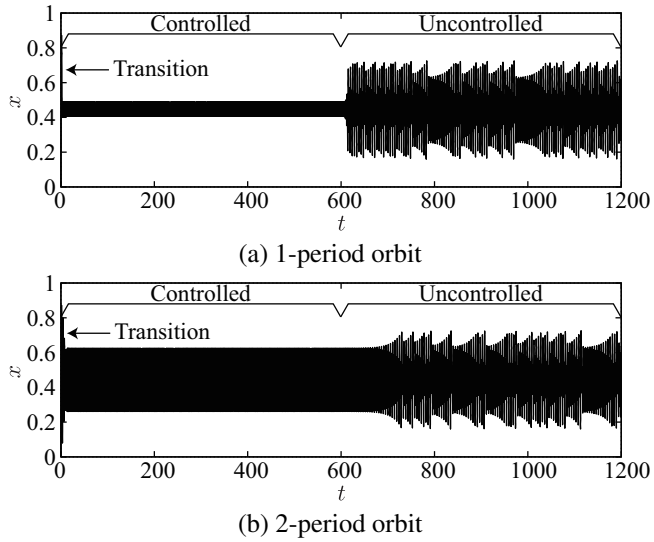

(a) 1-period orbit

(b) 2-period orbit

Figure 7: Long-time responses of the capacitor voltage. Note that the stabilization controlling is stop at $t = 600$. The model shows chaotic attractors after stopping the stabilization of UPOs.

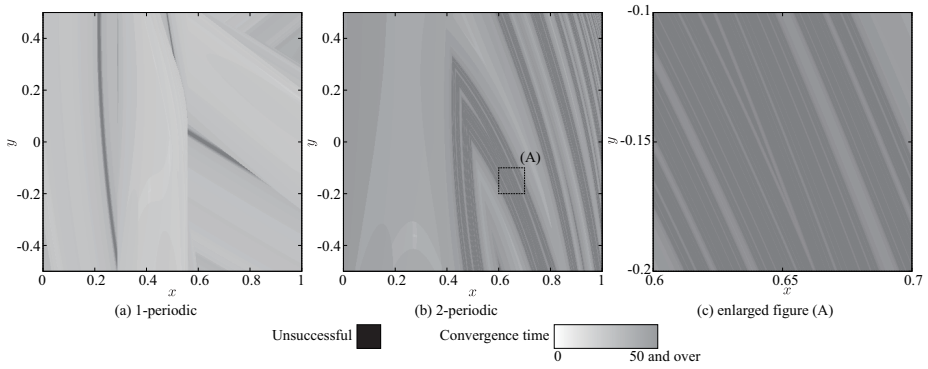

Figure 8: Basins of attraction. The black regions are unsuccessful initial points. Gray colors indicate elapsed times for convergence to UPOs. It is confirmed that all initial points can be controlled for objective UPOs.

5. Circuit implementation

We implemented the synchronous buck converter and proposed control circuits for laboratory experiments. Figure 9 shows the circuit diagram. A dead-time is included into the gate driver circuit with an LTC4440. The dead-time is the period at which two MOS-FETs turn off for preventing shoot-through current. Toshiba MOS-FET 2SK4017s are used for the switches. The load is regarded as a constant resistor, and E as an ideal voltage source.

The lower circuit in Fig. 9 is the control module of the converter. The controller is based on voltage-mode control. It is driven by the clock pulse input E_{pulse} that is generated by the microcomputer LPC4088. The LPC4088 has an analog-to-digital converter and can monitor the output voltage v_a and the inductor current i. The frequency of E_{pulse} is modulated depending on these values. Table 2 lists the specifications of the

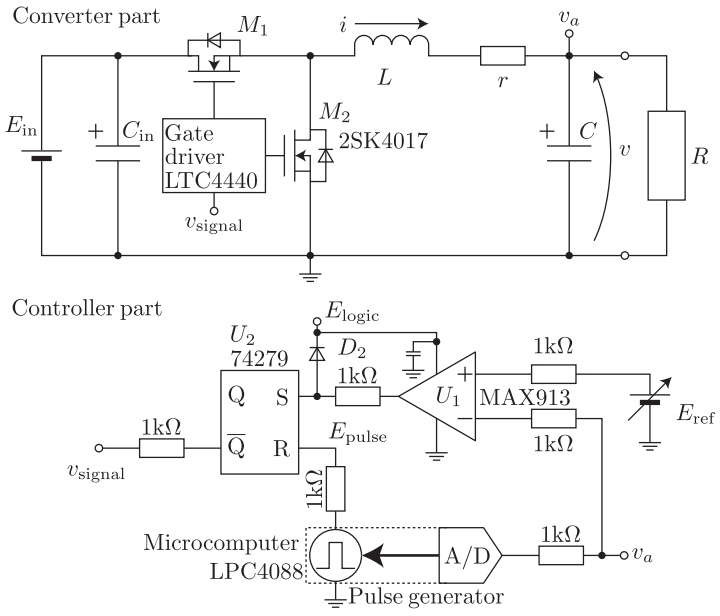

Figure 9: Circuit diagram of the converter and control part.

buck converter.

Figure 10 shows our experimental results. Channels 1 and 2 are clock pulses and output capacitor voltages, respectively. Especially, Fig 10 (c) is the time waveform of

Table 2: Specifications of the synchronous buck converter.

Source voltage E_{in}	12V
Reference voltage E_{ref}	1.1V
Inductor L	395.8μH
Series resistor of inductor r_L	1.129Ω
Output capacitor C	79.32μF
Series resistor of capacitor r_C	0.7924Ω
Load resistor R	100Ω
Switching frequency F	4.4kHz

capacitor voltages over a long period. Note that, in the first half of this plot, the circuit was controlled by the prototype controller. In the center of the figure, the control scheme changes to voltage-mode control without PFM.

The objective circuit behaves as a chaotic attractor without the stabilizing controller. In this case, the output ripple voltage fluctuates aperiodically. On the other hand, our controller can stabilize the 3-period attractor embedded into the chaotic behavior. Figure 10 (b) confirms that the capacitor voltage takes the 3-period waveform. Note that, in these two figures, the frequencies are equal, and they are close to 4.38kHz. Thus, our controller can stabilize UPOs but does not influence the original pulse frequency f. This circuit stabilizes the objective trajectory with small perturbations. Therefore, if the control input is removed, the circuit can no longer preserve its trajectory (see Fig. 10 (c)).

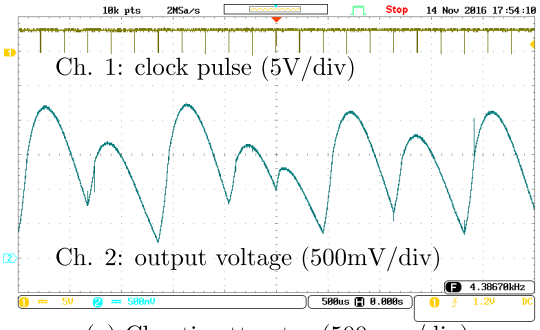

(a) Chaotic attractor (500μsec/div)

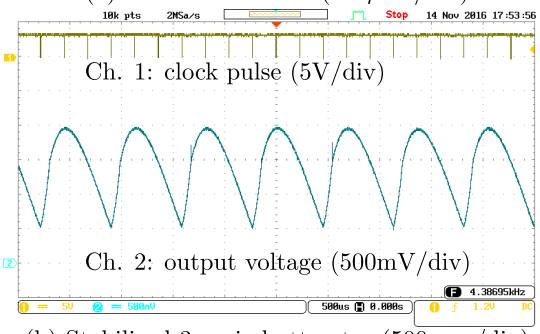

(b) Stabilized 3-period attractor (500μsec/div)

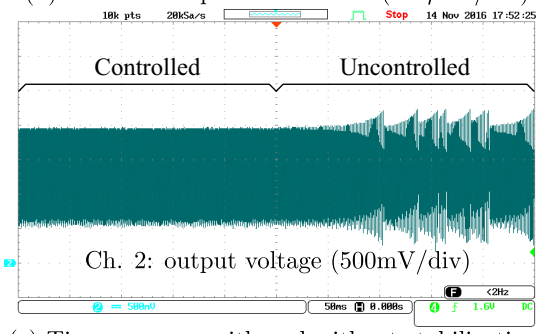

(c) Time response with and without stabilization (50msec/div)

Figure 10: Laboratory experiments. The converter without the proposed controller shows the chaotic attractor (a). The proposed controller can stabilize the embedded unstable 3-period attractor, and avoid the chaotic attractor (b).

6. Conclusion

In this paper, we have proposed a chaos-control scheme with PFM for synchronous buck converters, and we demonstrated its efficacy numerically and experimentally.

In switching converters, the frequency of PWM signals influences the circuit's behavior; so frequency modulation can control the circuit state. First, we described a normalized mathematical model and switching rules for the MOS-FET components. The switching threshold values were varied depending on the capacitor voltages and the inductor currents with their series resistors. Hence, the switching rule is described as the linear limit set $x > ay + b$. Next, we considered the pole-assignment method with limitations. To simplify the feedback controller, we derived the condition of dimension reduction for the controlling gain vector. As a result, the proposed method can control the circuit with only information about the output voltage values. Finally, we demonstrated the proposed controller for synchronous buck converters. The proposed method can stabilize objective UPOs without influencing the operative value E_{ref}. From experimental results and the basins of attraction they demonstrated, the effectiveness and robustness of our proposed method is demonstrated, since the state variables x and y of the circuit converge to UPOs from nearly all initial states.

Acknowledgment

This work was supported by JSPS KAKENHI Grant Number 16K18107.

References

[1] R. I. Leine, H. Nijmeijer, Dynamics and Bifurcations of Non-Smooth Mechanical Systems, Vol. 18 of Lecture Notes in Applied and Computational Mechanics, Springer Berlin Heidelberg, Berlin, Heidelberg, 2004. doi:10.1007/978-3-540-44398-8.
URL http://link.springer.com/10.1007/978-3-540-44398-8

[2] M. Djemai, M. Defoort (Eds.), Hybrid Dynamical Systems, Vol. 457 of Lecture Notes in Control and Information Sciences, Springer International Publishing,

Cham, 2015. doi:10.1007/978-3-319-10795-0.
URL http://link.springer.com/10.1007/978-3-319-10795-0

[3] M. Bernardo, C. Budd, A. R. Champneys, P. Kowalczyk, Piecewise-smooth Dynamical Systems, Vol. 163 of Applied Mathematical Sciences, Springer London, London, 2008. doi:10.1007/978-1-84628-708-4.

[4] K. Aihara, H. Suzuki, Theory of hybrid dynamical systems and its applications to biological and medical systems, Phil. Trans. R. Soc. A 368 (1930) (2010) 4893 LP – 4914.
URL http://rsta.royalsocietypublishing.org/content/368/1930/4893.abstract

[5] T. Saito, M. Oikawa, K. Jinno, Dynamics of hysteretic neural networks, in: IEEE, Proc. ISCAS 1991, Vol. 3, 1991, pp. 1469–1472. doi:10.1109/ISCAS.1991.176652.

[6] K. Kohari, T. Saito, H. Kawakami, On a Hysteresis Oscillator including Periodic Thresholds, IEICE Trans. Fundamentals E76-A (12) (1993) 2102—-2107.

[7] T. Inagaki, T. Saito, Consistency in a chaotic spiking oscillator, IEICE Trans. Fundamentals E91-A (8) (2008) 2240–2243. doi:10.1093/ietfec/e91-a.8.2240.

[8] D. C. Hamill, D. J. Jeffries, Subharmonics and chaos in a controlled switched-mode power converter, IEEE Trans. Circuits and Systems 35 (8) (1988) 1059–1061. doi:10.1109/31.1858.

[9] C. K. Tse, M. Di Bernardo, Complex behavior in switching power converters, in: Proc. IEEE, Vol. 90, 2002, pp. 768–781. doi:10.1109/JPROC.2002.1015006.
URL http://ieeexplore.ieee.org/lpdocs/epic03/wrapper.htm?arnumber=1015006

[10] G. Yuan, S. Banerjee, E. Ott, J. A. Yorke, Border-collision bifurcations in the buck converter, IEEE Trans. Circuits and Systems I 45 (7) (1998) 707–716. doi:10.1109/81.703837.

[11] A. E. Aroudi, D. Fournier, Bifurcation Behavior in a Two-Loop DC-DC Quadratic Boost Converter, in: IEEE, Proc. ISCAS 2015, 2015, pp. 2489–2492.

[12] J. H. B. Deane, D. C. Hamill, Improvement of power supply EMC by chaos, Electron. Lett. 32 (12) (1996) 1045–. doi:10.1049/el:19960716.

[13] E. Ott, C. Grebogi, J. A. Yorke, Controlling chaos, Phys. Rev. Lett 64 (1990) 1196–1199.

[14] K. Pyragas, Continuous control of chaos by self-controlling feedback, Phys. Lett. A 170 (6) (1992) 421–428. doi:10.1016/0375-9601(92)90745-8.
URL http://www.sciencedirect.com/science/article/pii/0375960192907458

[15] T. Kousaka, T. Ueta, H. Kawakami, Controlling chaos in a state-dependent nonlinear system, Int. J. Bifurcation and Chaos 12 (05) (2002) 1111–1119. doi:10.1142/S0218127402004942.

[16] D. Ito, T. Ueta, T. Kousaka, J. Imura, K. Aihara, Controlling Chaos of Hybrid Systems by Variable Threshold Values, Int. J. Bifurcation and Chaos 24 (10) (2014) 1450125. doi:10.1142/S0218127414501259.

[17] T. Sasada, D. Ito, T. Ueta, H. Ohtagaki, T. Kousaka, H. Asahara, Controlling Unstable Orbits via Varying Switching Time in a Simple Hybrid Dynamical Systems, in: IEICE, Proc. NOLTA 2015, 2015, pp. 475–478.

[18] N. Zamani, M. Ataei, M. Niroomand, Analysis and control of chaotic behavior in boost converter by ramp compensation based on Lyapunov exponents assignment: theoretical and experimental investigation, Chaos, Solitons & Fractals 81 (2015) 20–29. doi:10.1016/j.chaos.2015.08.010.

[19] Z. Yan-Li, L. Xiao-Shu, C. Guan-Rong, Pole placement method of controlling chaos in DC-DC buck converters, Chinese Physics 15 (8) (2006) 1719.
URL http://stacks.iop.org/1009-1963/15/i=8/a=015

[20] E. Rodríguez, E. Alarcón, H. H. C. Iu, A. E. Aroudi, A frequency domain approach for controlling chaos in switching converters, in: IEEE, Proc. ISCAS 2010, 2010, pp. 2928–2931. doi:10.1109/ISCAS.2010.5538031.

[21] H. Wu, V. Pickert, D. Giaouris, Nonlinear analysis for interleaved boost converters based on Monodromy matrix, in: IEEE, Proc. ECCE 2014, 2014, pp. 2511–2516. doi:10.1109/ECCE.2014.6953735.

[22] G. Poddar, K. Chakrabarty, S. Banerjee, Experimental control of chaotic behavior of buck converter, IEEE Trans. Circuits and Systems I 42 (8) (1995) 502–504. doi:10.1109/81.404067.

[23] P. Bryant, K. Wiesenfeld, Suppression of period-doubling and nonlinear parametric effects in periodically perturbed systems, Phys. Rev. A 33 (4) (1986) 2525–2543. doi:10.1103/PhysRevA.33.2525.
URL http://link.aps.org/doi/10.1103/PhysRevA.33.2525

[24] K. Wiesenfeld, B. McNamara, Small-signal amplification in bifurcating dynamical systems, Phys. Rev. A 33 (1) (1986) 629–642. doi:10.1103/PhysRevA.33.629.
URL http://link.aps.org/doi/10.1103/PhysRevA.33.629

[25] T. Shinbrot, C. Grebogi, J. A. Yorke, E. Ott, Using small perturbations to control chaos, Nature 363 (6428) (1993) 411–417.
URL http://dx.doi.org/10.1038/363411a0

[26] N. Kikuchi, Y. Liu, J. Ohtsubo, Chaos control and noise suppression in external-cavity semiconductor lasers, IEEE J. Quantum Electronics 33 (1) (1997) 56–65. doi:10.1109/3.554888.

[27] D. Ito, Chaos controlling with clock pulse modulation for dc-dc converter circuit, in: IEICE, Proc. NOLTA 2016, 2016, pp. 71–74.

[28] T. Ueta, H. Kawakami, Composite Dynamical System for Controlling Chaos, IEICE Trans. Fundamentals 78 (6) (1995) 708–714.
URL http://ci.nii.ac.jp/naid/110003215992/

[29] H. Kawakami, Bifurcation of periodic responses in forced dynamic nonlinear circuits: Computation of bifurcation values of the system parameters, IEEE Trans. Circuits and Systems 31 (3) (1984) 248–260. doi:10.1109/TCS.1984.1085495.

[30] Y. Miino, D. Ito, T. Ueta, A computation method for non-autonomous systems with discontinuous characteristics, Chaos, Solitons & Fractals 77 (2015) 277–285. doi:10.1016/j.chaos.2015.06.014.